

# Extending the fair sampling assumption using causal diagrams

Valentin Gebhart and Augusto Smerzi

QSTAR, INO-CNR and LENS, Largo Enrico Fermi 2, 50125 Firenze, Italy

**Discarding undesirable measurement results in Bell experiments opens the detection loophole that prevents a conclusive demonstration of nonlocality. As closing the detection loophole represents a major technical challenge for many practical Bell experiments, it is customary to assume the so-called fair sampling assumption (FSA) that, in its original form, states that the collectively postselected statistics are a fair sample of the ideal statistics. Here, we analyze the FSA from the viewpoint of causal inference: We derive a minimal causal diagram that encapsulates the FSA. This provides an easy, intuitive, and unifying approach that includes different accepted forms of the FSA. We show that the FSA can not only be applied in scenarios with non-ideal detectors or transmission losses, but also in ideal experiments where only parts of the correlations are postselected, e.g., when the particles' destinations are in a superposition state. Finally, we demonstrate that the FSA is also applicable in multipartite scenarios that test for (genuine) multipartite nonlocality.**

## 1 Introduction

Bell nonlocality [1, 2] represents one of the central pillars of modern research in quantum foundations and the development of quantum technologies [3]. A widely used technique in Bell experiments is the discard of events of an incomplete detection such as, e.g., a non-detection of parts of the system due to particle losses. By the selection bias [4], the postselection opens the detection loophole, i.e., the possibility of a local hidden variable (LHV) model to describe the observed correlations even if postselected correlations violate Bell inequality [5, 6]. The detection loophole is not just conspiratorial: It was used

in experiments to create fake violations of Bell inequalities [7, 8, 9, 10].

Ideally, one can close the detection loophole by including the non-detection events [6, 11, 12, 13] or by sharpening the Bell inequalities [14, 15]. These methods require high detection efficiencies and have recently been implemented in sophisticated Bell experiments that close the detection loophole [16, 17, 18] (also while simultaneously closing the locality loophole [19, 20, 21]). However, the required detection efficiencies represent a severe technical challenge for the practicality of Bell experiments. Thus, a widely-used way out is to rely on the fair sampling assumption (FSA) [22, 6, 23, 24] that is commonly known as the assumption that the postselected statistics is a fair representation of (i.e., is identical to) the statistics that would have been observed using perfect detectors and no losses. An alternative form of the FSA is the assumption that the detector settings have no influence on the detection probability of the particles. In the latter case, the postselected statistics is not identical to the statistics that would be observed with ideal detectors but, nonetheless, the postselection cannot create any fake nonlocal correlations. Due to the high technical requirements of closing the detection loophole (e.g., optimal detectors and minimal transmission losses), the FSA is still widely used in Bell experiments [25, 26, 27, 28, 29, 30, 31].

In this work, we analyze the FSA from the viewpoint of causal inference and causal diagrams [4]. In particular, we ask how the causal diagram of a Bell experiment must be (minimally) altered to allow for a valid demonstration of nonlocality even after a collectively decided postselection: The diagram should guarantee that the postselection cannot create fake nonlocal correlations due to the selection bias. Importantly, we ensure that the causal diagram provides a meaningful description of the experiment by dis-

allowing any kind of fine-tuning of causal influences [4, 32, 33], in contrast to previous studies of the FSA. This results in an easy and intuitive way to understand different forms of the FSA found in the literature. Furthermore, we show that the such-obtained causal-diagram FSA can be applied to different experiments where the correlations must be postselected even in the ideal noiseless setup, and not just in the standard setup with non-ideal detectors and particle losses. Finally, we prove that the FSA is also useful in experiments that demonstrate multipartite nonlocality and genuine multipartite nonlocality.

## 2 Fair sampling in the bipartite scenario

In the following, we derive a minimal extension of the causal diagram of the bipartite Bell scenario, Fig. 1(a), that allows a collective postselection, Fig. 1(b), without potentially creating fake correlations that violate the Bell inequality. The central promise is to have a causal description that does not employ any fine-tuning of its causal influences. By a fine-tuning of the parameters of a causal model, two variables can be made statistically independent even though they seem to affect each other in the causal diagram. Instead, without fine-tuning, any statistical independence between two variables must be evident from the diagram's structure. If one allows for fine-tuning, the description in terms of causal diagram becomes irrelevant [4, 32, 33] because any statistical (in)dependence can just be directly imposed by hand.

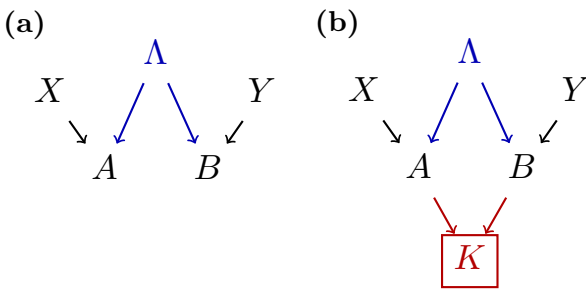


Figure 1: (a) The causal diagram of the local hidden variable (LHV) model in the standard bipartite Bell scenario. (b) A collective postselection is indicated as the variable  $K$  that is influenced by both Alice's outcome  $A$  and Bob's outcome  $B$ , opening the detection loophole by the selection bias [5].

The central tool to infer independencies from a causal diagram are the  $d$ -separation rules [4] that dictate whether a given path connecting two variables of the causal diagram is open (i.e., the variables are generally dependent) or blocked (the variables must be independent), also when conditioning on other variables of the diagram. The rules state that (i) a path is blocked if along it there is a collider (a variable where two causal arrows collide), (ii) a path is blocked if along it there is a non-collider that is conditioned on, and (iii) a path is open if along it there is a collider and we condition on the collider or its descendants. The last rule manifests itself in the selection bias and the Berkson paradox [4]. We want to note that in the context of Bell experiments, causal diagrams and the  $d$ -separation rules have been used to show that quantum violations of Bell inequalities require fine-tuning in classical-causal explanations (e.g., superdeterminism, superluminal influences, or retrocausal influences) [33, 34, 35], and to show that certain collective postselection strategies are safe for the demonstration of multipartite nonlocality [36] and genuine multipartite nonlocality [37].

In the standard bipartite Bell scenario, two parties, Alice and Bob, share the two parts of a quantum system and each perform local measurements on their subsystem. Alice (Bob) chooses the measurement setting  $x$  ( $y$ ) and records the measurement outcome  $a$  ( $b$ ). The measured correlations are called local if they can be described by a LHV model of the form [1, 2]

$$p_{ab|xy} = \sum_{\lambda} p_{\lambda} p_{a|x\lambda} p_{b|y\lambda}, \quad (1)$$

where  $p_{\lambda}$ ,  $p_{a|x\lambda}$ , and  $p_{b|y\lambda}$  are (conditional) probabilities, each summing to 1, e.g.,  $\sum_{\lambda} p_{\lambda} = 1$ . The corresponding causal diagram is shown in Fig. 1(a). Using Eq. (1), one can derive Bell inequalities, a violation of which proves that the correlations are nonlocal.

In Fig. 1(b), we include the variable  $K$  representing the decision of the collective postselection (e.g.,  $K = 1$  for postselecting the results and  $K = 0$  for discarding the results). For a valid postselection, the postselected statistics (i.e., the correlations  $p_{ab|xyk}$  conditioned on a specific postselection value  $K = k$ ) must be of the form of a LHV model as Eq. (1). Using  $p_{ab|xyk} = \sum_{\lambda} p_{\lambda|xyk} p_{ab|xy\lambda k}$ , we obtain the two

conditions

$$\mathbf{CI} : \quad p_{\lambda|xyk} = p_{\lambda|k}$$

$$\mathbf{CII} : \quad p_{ab|xy\lambda k} = p_{a|x\lambda k} p_{b|y\lambda k}$$

that ensure a valid postselection. We now consider a postselection that is collective: Both parties must consult each other to decide the postselection. Note that if each party can decide the postselection locally, there is no need for a FSA because the postselection is known to be safe [13, 36]. Therefore, in the causal diagram,  $K$  is influenced by the both measurement outcomes  $A$  and  $B$ <sup>1</sup>, see Fig. 1(b). However, a postselection described by the causal diagram in Fig. 1(b) is in conflict with condition **CI**: There is an open path  $X \rightarrow A \rightarrow K \leftarrow B \leftarrow \Lambda$  ( $K$  is a collider that is conditioned on), which contradicts  $p_{\lambda|xyk} = p_{\lambda|k}$ .

The causal diagram of Fig. 1(b) can thus not give a causal account of the fair sampling without employing a fine-tuning of causal influences. How must one alter the diagram for a valid explanation? We first note that including further unobserved or hidden variables in the diagram cannot solve the problem<sup>2</sup>. Also when adding more setting variables that influence the measurement outcomes, the above path remains open. Thus, in order to proceed, the first divide the outcome variables  $A$  into  $(A_1, A_2)$  and  $B$  into  $(B_1, B_2)$ , where only the values of  $A_1$  and  $B_1$  are fed into the Bell inequality. In the general case, all variables are again influenced by the respective setting and the LHV  $\Lambda$  and influence the postselection  $K$ . Furthermore, there may be arbitrary influences between  $A_1$  and  $A_2$  which we indicate as a bidirected arrow with circular endings, including  $A_1 \rightarrow A_2$ ,  $A_1 \leftarrow A_2$ , or the existence

<sup>1</sup>Strictly speaking, a collective postselection could also include direct influences from the settings  $X$  and  $Y$  to  $K$ , e.g., in a postselection influenced only by  $X$  and  $B$ , or only by  $X$  and  $Y$ . A postselection influenced by  $X$  and  $B$  leads to a conflict with condition **CI**, similar a postselection influenced by  $A$  and  $B$  as in the main text. On the other side, a postselection that is decided only by  $X$  and  $Y$  is a safe postselection, i.e., the conditions **CI** and **CII** still hold. This can be seen by noting that, if  $K$  is influenced only by  $X$  and  $Y$ , one simply has  $p_{ab|xyk} = p_{ab|xy}$ .

<sup>2</sup>For instance, the inclusion of a variable  $\Gamma$  between  $X$  and  $A$  either blocks the dependence between  $X$  and  $A$  if  $\Gamma$  is a collider ( $X \rightarrow \Gamma \leftarrow A$ ), in which case there would be no influence from Alice's setting  $X$  to her outcome  $A$ , or, otherwise, the path  $X \leftrightarrow \Gamma \leftrightarrow A \rightarrow K \leftarrow B \leftarrow \Lambda$ , with  $\Lambda$  being a non-collider, remains open.

of a hidden variable  $\Gamma$  such that  $A_1 \leftarrow \Gamma \rightarrow A_2$  (a hidden common cause), and combinations of thereof. Note that a hidden common cause can be included in the LHV  $\Lambda$ . The corresponding causal structure is depicted in Fig. 2(a).

This general causal structure does not fulfill the conditions of valid postselection for the same reasons as above. We now derive the most general simplification of Fig. 2(a) that fulfills the conditions of a valid postselection without requiring fine-tuning. Since the variables  $A_1$  and  $B_1$  are inserted in the Bell inequality, and we must have  $X \rightarrow A_1$ ,  $Y \rightarrow B_1$ ,  $\Lambda \rightarrow A_1$ , and  $\Lambda \rightarrow B_1$  to describe nontrivial correlations that depend on the measurement settings, we must have that  $A_1 \not\rightarrow K$  and  $B_1 \not\rightarrow K$  to fulfill condition **CI**. This is because, if, e.g.,  $A_1 \rightarrow K$ , the path  $X \rightarrow A_1 \leftarrow \Lambda$  would be open because we condition on  $K$ , a descendant of the collider  $A_1$ . Next, if one had an influence  $A_1 \rightarrow A_2$ , there would be an open path  $X \rightarrow A_1 \rightarrow A_2 \rightarrow K \leftarrow B_2 \leftarrow \Lambda$ , again violating condition **CI**. The same holds true for a possible dependence between  $B_1$  and  $B_2$ . Also, if one had  $A_2 \rightarrow A_1$  and  $B_2 \rightarrow B_1$ , there would be an open path  $A_1 \leftarrow A_2 \rightarrow K \leftarrow B_2 \rightarrow B_1$ , in conflict with condition **CII**. Thus, we arrive at the causal diagram of Fig. 2(b).

Since we consider a collective postselection, we exclude the cases  $A_2 \not\rightarrow K$  or  $B_2 \not\rightarrow K$ . Furthermore, we also dismiss the case that  $\Lambda \not\rightarrow A_2$  and  $\Lambda \not\rightarrow B_2$ , in which case  $K$  would only depend on  $X$  and  $Y$  and the postselection would trivially valid<sup>1</sup>. Therefore, taking, e.g.,  $\Lambda \rightarrow A_2$ , we must have  $Y \not\rightarrow B_2$  because, otherwise, there would be an open path  $\Lambda \rightarrow A_2 \rightarrow K \leftarrow B_2 \leftarrow Y$ , and we also have  $X \not\rightarrow A_2$  because, otherwise, there would be an open path  $X \rightarrow A_2 \leftarrow \Lambda$  ( $K$  is a descendant of  $A_2$ ), both of which would be in conflict with condition **CI**. We thus we arrive at the causal diagram of Fig. 2(c).

Using the causal diagram of Fig. 2(c), one can finally check the validity of conditions **CI** and **CII**: For instance, for proving that  $p_{\lambda|zk} = p_{\lambda|k}$ , note that the only path connecting  $X$  and  $\Lambda$  passes through  $A_1$  that, being a collider, blocks the path. For showing that  $p_{a_1b_1|xy\lambda k} = p_{a_1|x\lambda k} p_{b_1|y\lambda k}$  note that the only paths that connect  $A_1$  and  $X$  to  $B_1$  and  $Y$  pass through  $\Lambda$ , and are blocked because  $\Lambda$  is a non-collider that is conditioned on.

Above, we have derived the a minimal extension of the bipartite causal diagram that allows

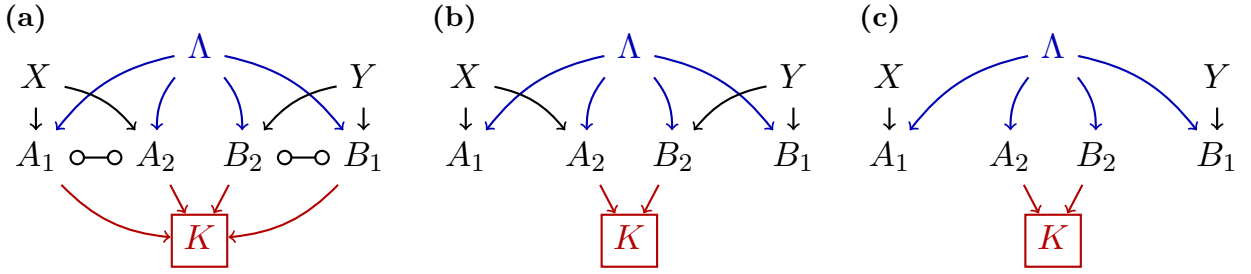


Figure 2: Causal diagrams of the minimal extension of the bipartite causal diagram accounting for the fair sampling assumption (FSA). (a) Most general causal diagram in the bipartite case with two measurement outcomes per party. The outcomes of each party can be connected by an unknown causal influence as indicated as the bidirected arrows. (b) The causal diagram after the elimination of all causal influences connected to  $A_1$  and  $B_1$  (i.e., to the outcomes that are used for the Bell inequality) that are in conflict with the conditions for safe postselection. (c) The final fair-sampling causal diagram after the elimination of all causal influences connected to  $A_2$  and  $B_2$  that are in conflict with the conditions for safe postselection.

a demonstration of nonlocality after a collective postselection, describing a general FSA for collective postselection. However, the typical application of the FSA are situations in which each measurement party needs to detect a single particle. Here, the variables  $A_2$  and  $B_2$  correspond to the number of detected particles in Alice's and Bob's experiment, respectively. This is a special case of a collective postselection, in which post-selecting an event (e.g., denoted as  $K = 1$ ) is equivalent to a fixed combination of values for  $A_2$  and  $B_2$  ( $A_2 = B_2 = 1$ ). Thus, one can simply use a causal diagram with a conditioning on the variables  $A_2$  and  $B_2$  without introducing the postselection variable  $K$ . While influences such as  $X \rightarrow A_2$  and  $A_1 \rightarrow A_2$  are still in conflict with condition **CI**, an influence of the form  $A_2 \rightarrow A_1$  can now be allowed. The corresponding causal diagram is shown in Fig. 3. The causal diagram of Fig. 2(c) is more general though: An example of a collective postselection that cannot be modeled with Fig. 3 is when the parties postselect events for which  $A_2 = B_2$ . Here, a postselected event does not imply fixed values of  $A_2$  and  $B_2$ .

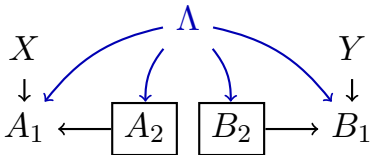


Figure 3: A possible causal diagram for the FSA if, for the postselection of the results, each party must receive a single particle. Here,  $A_2$  ( $B_2$ ) corresponds to the number of particles detected in Alice's (Bob's) measurement device.

We want to emphasize that the causal-diagram FSA is not only applicable to the standard scenario where one particle is sent to each party but there are detection and transmission losses, but also for certain postselection methods if the particles are generated in a superposition of their destinations [38, 39, 13]. In particular, demonstrations that a coincidence postselection is safe if the number of particles is conserved [36, 37] become unnecessary if one assumes the FSA. In other words, the FSA covers both a postselection due to inefficient detectors and transmission losses, and a postselection in ideal experiments due to a varying distribution of particles.

To conclude this section, we want to mention a setup proposed by Franson [40] to create nonlocality from energy-time entanglement. However, in this proposal, due to the selection bias, one can find a LHV model that reproduces the observed statistics and the apparent Bell inequality violation [41, 42]. Here, each party has two different measurement outcomes, an early detection time and a late detection time. Even in the ideal noiseless case, the statistics must be collectively postselected in order to violate a Bell inequality: Only events are postselected for which both particles arrive either at the early or at the late detection time. In this case, there is no way to introduce two different variables per party, e.g.,  $A_1$  and  $A_2$  as above, of which one is used in the postselection and one is used for the Bell inequality. This is because, for both the postselection and the Bell inequality, the crucial information is the time of arrival. Thus, the original Franson setup [40] cannot be validated for nonlocality demonstrations

with the causal-diagram FSA, and one must alter the experimental setup to generate nonlocality from energy-time entanglement [43, 44].

## 2.1 Comparison to standard FSAs

We now want to briefly compare the causal-diagram FSA to its different forms found in the literature. We emphasize that any of the following forms of the FSA corresponds to a fine-tuning condition on the original causal diagram of the Bell experiment (Fig. 1). We first comment on the common (mis-)understanding that the FSA means that there is no observable influence of the measurement setting on the probability of detecting a particle,  $p_{d|x} = p_d$ , where  $d$  represents Alice's detection of a particle. As shown in Ref. [23] with a counter example, this assumption does not ensure a safe postselection. The original way of stating the FSA is that the postselected statistics should be a fair sample of (i.e., be identical to) the statistics that would have been obtained using perfect detectors [6]. This assumption is satisfied if  $p_{d|x\lambda} = p_d$ , i.e., if the probability of detecting a particle depends neither on the setting  $X$  nor on the LHV  $\Lambda$ . This condition ensures a safe postselection but, as we have seen above, can be weakened: assuming that  $p_{d|x\lambda} = p_{d|\lambda}$  already provides a safe postselection [23]. Here, the postselected ensemble may differ from the original one,  $p_{\lambda|k} \neq p_\lambda$ , but it still has the form of a LHV model, Eq. (1). Assuming a causal-diagram representation without fine-tuning, the assumption that  $X$  cannot influence the detection variable corresponds to the above causal diagrams of Fig. 2(c) or Fig. 3.

Finally, we note that this FSA can be further weakened to the assumption that  $p_{d|x\lambda} = \eta_x^{(d)} \eta_\lambda^{(d)}$  [23, 24], i.e., the assumption that the detection efficiency depends on both the setting  $X$  and the LHV  $\Lambda$  but it factorizes. This factorization condition cannot be depicted in a causal diagram and, as the dependence implies that  $A_2$  is influenced by both  $X$  and  $\Lambda$ , it represents a fine-tuning of the causal influences.

## 3 Fair sampling for genuine multipartite nonlocality

The causal-diagram FSA of Fig. 2(c) (or Fig. 3) is also sufficient to validate a collective postselec-

tion in a multipartite Bell experiment. For more than two measurement parties, there are different notions of nonlocality that can be demonstrated by a violation of the corresponding inequalities [45, 46, 47, 48]. For simplicity, we focus on the three-partite case, but the discussion holds for any number of parties. We thus include a third party Charlie who chooses a measurement setting  $z$  and observes the measurement outcomes  $(c_1, c_2)$ . First, one can assume a LHV model in the multipartite case similar to Eq. (1), corresponding to a causal structure as shown in Fig. 4(a), where we included the FSA derived above. Using the LHV model, one can demonstrate inequalities that test multipartite nonlocality [46]. The validity of the postselection, namely the conditions  $p_{\lambda|xyzk} = p_{\lambda|k}$  and  $p_{a_1b_1c_1|xyz\lambda k} = p_{a_1|x\lambda k} p_{b_1|y\lambda k} p_{c_1|z\lambda k}$ , can be shown in exact analogy to the bipartite case above.

A second and stronger form of three-partite nonlocality is genuine three-partite nonlocality. Here, instead of assuming a LHV model, one allows for two of the three parties to share nonlocal quantum correlations, in a model that is called a hybrid local-nonlocal hidden variable model [45]. These quantum correlations, fulfilling the no-signalling principle [48], cannot be depicted in a classical causal diagram without using fine-tuning conditions [33, 34]. In Fig. 4, we indicate these correlations as light blue lines between the outcome variables, reminding that these influences are subject to the no-signalling principle. The hybrid model then dictates that, given a specific hidden variable  $\lambda$  (i.e., when conditioning on  $\Lambda$ ), there can only be nonlocal correlations between two of the parties, see Fig. 4(c). In contrast, when not conditioning on  $\Lambda$ , there can possibly exist nonlocal correlations between any pair of parties, see Fig. 4(b), where we use different colors to emphasize that only one pair of the parties can share nonlocal correlations at a time.

Hybrid local-nonlocal hidden variable models fulfill certain inequalities that test for genuine multipartite nonlocality [45], and, similar to above, there are conditions on the postselected statistics that, if fulfilled, prove that a collective postselection is safe [37]. One can directly show that, using the causal-diagram FSA as shown in Fig. 4, the conditions of a safe postselection are fulfilled. For instance, for the first condition,  $p_{\lambda|xyzk} = p_{\lambda|k}$ , we note that a path

such as  $X \rightarrow A_1 \rightarrow B_2 \rightarrow K \leftarrow C_2 \leftarrow \Lambda$ , that appears to be an open path since the collider  $K$  is conditioned on, is blocked due to the no-signalling condition: Alice's measurement setting  $X$  cannot influence Bob's measurement outcome  $B_2$ . The validity of the second condition of a factorization given a specific value of  $\Lambda$ , e.g.,  $p_{a_1 b_1 c_1 | xyz \lambda k} = p_{a_1 b_1 | xyz \lambda k} p_{c_1 | z \lambda k}$ , see Fig. 4(c), can again be seen by noting that any path that connects  $C_1$  and  $Z$  to the other parties passes through  $\Lambda$ , and is thus blocked because  $\Lambda$  is a non-collider that is conditioned on. Thus we see that the FSA depicted in Fig. 4 also suffices to validate a collective postselection for the demonstration of genuine multipartite nonlocality.

Finally, as in the bipartite case, if each party needs to measure a single particle, the FSA can also be explained by a three-partite causal diagram similar to Fig. 3. Here,  $A_2$  represents the number detected particles in Alice's measurement, and one can allow for an influence of the form  $A_2 \rightarrow A_1$ , and similarly for Bob and Charlie. Also this version of a fair-sampling causal diagram suffices to prove the conditions of a safe postselection for both multipartite nonlocality and genuine multipartite nonlocality.

## 4 Conclusions

We have discussed a causal explanation of the fair sampling assumption (FSA) that ensures that a collective postselection cannot create fake nonlocal correlations in Bell experiments. For this purpose, we have derived a minimal extension of the causal diagram of the bipartite Bell scenario that guarantees that the postselected statistics take the form of a local hidden variable (LHV) model, without requiring a fine-tuning of the causal influences. We have employed the framework of causal inference and  $d$ -separation rules [4] as a mediator between a causal structure and the implied relations of conditional independence between the variables. The thus-obtained causal diagrams yield an easy and intuitive explanation of the FSA and can be used to understand different forms of the FSA of the literature. Furthermore, besides standard Bell scenarios with a non-ideal detection and particle losses, we have demonstrated that the causal-diagram FSA can also be applied in noise-free scenarios where the statistics must be postselected because the parti-

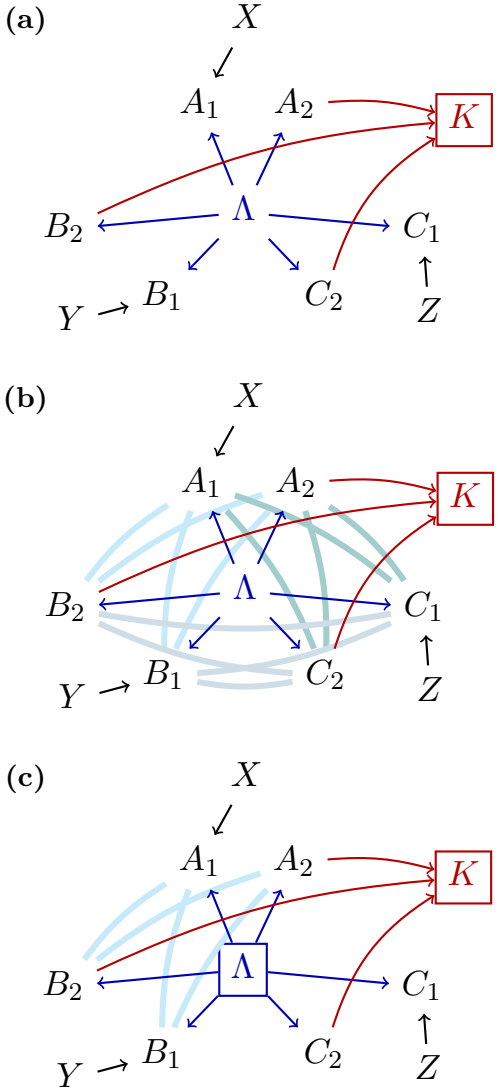


Figure 4: Causal diagrams of the FSA in the three-partite Bell scenario, for (a) a local hidden variable (LHV) model that corresponds to tests of multipartite nonlocality and (b,c) a hybrid local-nonlocal hidden variable model that corresponds to tests of genuine multipartite nonlocality. (c) In the hybrid model, when conditioning on a specific value of the LHV  $\Lambda$ , two of the three parties can share nonlocal quantum correlations (light blue lines) that are subject to the no-signalling fine-tuning condition.

cles are randomly distributed between the parties [38, 39, 37]. Finally, we have shown that the FSA also validates a collective postselection in demonstrations of multipartite nonlocality and genuine multipartite nonlocality.

## Acknowledgments

This work was supported by the European Commission through the QuantERA ERA-NET Cofund in Quantum Technologies project “MENTA”.

## References

- [1] John S Bell. “On the einstein podolsky rosen paradox”. *Physics* **1**, 195 (1964).
- [2] John S Bell. “The theory of local beables”. In *Speakable and Unspeakable in Quantum Mechanics: Collected Papers on Quantum Philosophy*. Pages 52–62. Cambridge University Press (2004). 2 edition.
- [3] Nicolas Brunner, Daniel Cavalcanti, Stefano Pironio, Valerio Scarani, and Stephanie Wehner. “Bell nonlocality”. *Rev. Mod. Phys.* **86**, 419–478 (2014).
- [4] Judea Pearl. “Causality: Models, reasoning, and inference”. Cambridge University Press. (2009).
- [5] Philip M. Pearle. “Hidden-variable example based upon data rejection”. *Phys. Rev. D* **2**, 1418–1425 (1970).
- [6] John F. Clauser and Michael A. Horne. “Experimental consequences of objective local theories”. *Phys. Rev. D* **10**, 526–535 (1974).
- [7] D. S. Tasca, S. P. Walborn, F. Toscano, and P. H. Souto Ribeiro. “Observation of tunable popescu-rohrlich correlations through postselection of a gaussian state”. *Phys. Rev. A* **80**, 030101 (2009).
- [8] Ilja Gerhardt, Qin Liu, Antía Lamas-Linares, Johannes Skaar, Valerio Scarani, Vadim Makarov, and Christian Kurtsiefer. “Experimentally faking the violation of bell’s inequalities”. *Phys. Rev. Lett.* **107**, 170404 (2011).
- [9] Enrico Pomarico, Bruno Sanguinetti, Pavel Sekatski, Hugo Zbinden, and Nicolas Gisin. “Experimental amplification of an entangled photon: what if the detection loophole is ignored?”. *New J. Phys.* **13**, 063031 (2011).
- [10] J Romero, D Giovannini, D S Tasca, S M Barnett, and M J Padgett. “Tailored two-photon correlation and fair-sampling: a cautionary tale”. *New J. Phys.* **15**, 083047 (2013).
- [11] N. David Mermin. “The epr experiment—thoughts about the “loophole””. *Ann. N. Y. Acad. Sci.* **480**, 422–427 (1986).
- [12] Philippe H. Eberhard. “Background level and counter efficiencies required for a loophole-free einstein-podolsky-rosen experiment”. *Phys. Rev. A* **47**, R747–R750 (1993).
- [13] Fabio Sciarrino, Giuseppe Vallone, Adán Cabello, and Paolo Mataloni. “Bell experiments with random destination sources”. *Phys. Rev. A* **83**, 032112 (2011).
- [14] Anupam Garg and N. D. Mermin. “Detector inefficiencies in the einstein-podolsky-rosen experiment”. *Phys. Rev. D* **35**, 3831–3835 (1987).
- [15] Jan-Åke Larsson. “Bell’s inequality and detector inefficiency”. *Phys. Rev. A* **57**, 3304–3308 (1998).
- [16] Mary A Rowe, David Kielpinski, Volker Meyer, Charles A Sackett, Wayne M Itano, Christopher Monroe, and David J Wineland. “Experimental violation of a bell’s inequality with efficient detection”. *Nature* **409**, 791–794 (2001).
- [17] D. N. Matsukevich, P. Maunz, D. L. Moehring, S. Olmschenk, and C. Monroe. “Bell inequality violation with two remote atomic qubits”. *Phys. Rev. Lett.* **100**, 150404 (2008).
- [18] B. G. Christensen, K. T. McCusker, J. B. Altepeter, B. Calkins, T. Gerrits, A. E. Lita, A. Miller, L. K. Shalm, Y. Zhang, S. W. Nam, N. Brunner, C. C. W. Lim, N. Gisin, and P. G. Kwiat. “Detection-loophole-free test of quantum nonlocality, and applications”. *Phys. Rev. Lett.* **111**, 130406 (2013).
- [19] Lynden K. Shalm, Evan Meyer-Scott, Bradley G. Christensen, Peter Bierhorst, Michael A. Wayne, Martin J. Stevens, Thomas Gerrits, Scott Glancy, Deny R. Hamel, Michael S. Allman, Kevin J. Coakley, Shellee D. Dyer, Carson Hodge, Adriana E. Lita, Varun B. Verma, Camilla Lambrocco, Edward Tortorici, Alan L. Migdall, Yanbao Zhang, Daniel R. Kumor, William H. Farr, Francesco Marsili, Matthew D. Shaw, Jeffrey A. Stern, Carlos Abellán, Waldimar Amaya, Valerio Pruneri, Thomas Jennewein, Morgan W. Mitchell, Paul G. Kwiat, Joshua C. Bienfang, Richard P. Mirin, Emanuel Knill, and

Sae Woo Nam. “Strong loophole-free test of local realism”. *Phys. Rev. Lett.* **115**, 250402 (2015).

[20] Marissa Giustina, Marijn A. M. Versteegh, Sören Wengerowsky, Johannes Handsteiner, Armin Hochrainer, Kevin Phelan, Fabian Steinlechner, Johannes Kofler, Jan-Åke Larsson, Carlos Abellán, Waldimar Amaya, Valerio Pruneri, Morgan W. Mitchell, Jörn Beyer, Thomas Gerrits, Adriana E. Lita, Lynden K. Shalm, Sae Woo Nam, Thomas Scheidl, Rupert Ursin, Bernhard Wittmann, and Anton Zeilinger. “Significant-loophole-free test of bell’s theorem with entangled photons”. *Phys. Rev. Lett.* **115**, 250401 (2015).

[21] Bas Hensen, Hannes Bernien, Anaïs E Dréau, Andreas Reiserer, Norbert Kalb, Machiel S Blok, Just Ruitenberg, Raymond FL Vermeulen, Raymond N Schouten, Carlos Abellán, et al. “Loophole-free bell inequality violation using electron spins separated by 1.3 kilometres”. *Nature* **526**, 682–686 (2015).

[22] John F. Clauser, Michael A. Horne, Abner Shimony, and Richard A. Holt. “Proposed experiment to test local hidden-variable theories”. *Phys. Rev. Lett.* **23**, 880–884 (1969).

[23] Dominic W. Berry, Hyunseok Jeong, Magdalena Stobińska, and Timothy C. Ralph. “Fair-sampling assumption is not necessary for testing local realism”. *Phys. Rev. A* **81**, 012109 (2010).

[24] Davide Orsucci, Jean-Daniel Bancal, Nicolas Sangouard, and Pavel Sekatski. “How post-selection affects device-independent claims under the fair sampling assumption”. *Quantum* **4**, 238 (2020).

[25] Igor Marinković, Andreas Wallucks, Ralf Riedinger, Sungkun Hong, Markus Aspelmeyer, and Simon Gröblacher. “Optomechanical bell test”. *Phys. Rev. Lett.* **121**, 220404 (2018).

[26] Dominik Rauch, Johannes Handsteiner, Armin Hochrainer, Jason Gallicchio, Andrew S. Friedman, Calvin Leung, Bo Liu, Lukas Bulla, Sebastian Ecker, Fabian Steinlechner, Rupert Ursin, Beili Hu, David Leon, Chris Benn, Adriano Ghedina, Massimo Cecconi, Alan H. Guth, David I. Kaiser, Thomas Scheidl, and Anton Zeilinger. “Cosmic bell test using random measurement settings from high-redshift quasars”. *Phys. Rev. Lett.* **121**, 080403 (2018).

[27] Emanuele Polino, Iris Agresti, Davide Poderini, Gonzalo Carvacho, Giorgio Milani, Gabriela Barreto Lemos, Rafael Chaves, and Fabio Sciarrino. “Device-independent test of a delayed choice experiment”. *Phys. Rev. A* **100**, 022111 (2019).

[28] S. Gómez, A. Mattar, I. Machuca, E. S. Gómez, D. Cavalcanti, O. Jiménez Farías, A. Acín, and G. Lima. “Experimental investigation of partially entangled states for device-independent randomness generation and self-testing protocols”. *Phys. Rev. A* **99**, 032108 (2019).

[29] Davide Poderini, Iris Agresti, Guglielmo Marchese, Emanuele Polino, Taira Giordani, Alessia Suprano, Mauro Valeri, Giorgio Milani, Nicolò Spagnolo, Gonzalo Carvacho, et al. “Experimental violation of n-locality in a star quantum network”. *Nat. Commun.* **11**, 1–8 (2020).

[30] Santiago Tarrago Velez, Vivishek Sudhir, Nicolas Sangouard, and Christophe Galland. “Bell correlations between light and vibration at ambient conditions”. *Sci. Adv.* **6**, eabb0260 (2020).

[31] Iris Agresti, Davide Poderini, Leonardo Guerini, Michele Mancusi, Gonzalo Carvacho, Leandro Aolita, Daniel Cavalcanti, Rafael Chaves, and Fabio Sciarrino. “Experimental device-independent certified randomness generation with an instrumental causal structure”. *Commun. Phys.* **3**, 1–7 (2020).

[32] Peter Spirtes, Clark N Glymour, Richard Scheines, and David Heckerman. “Causation, prediction, and search”. *MIT press*. (2000).

[33] Christopher J Wood and Robert W Spekkens. “The lesson of causal discovery algorithms for quantum correlations: causal explanations of bell-inequality violations require fine-tuning”. *New J. Phys.* **17**, 033002 (2015).

[34] John-Mark A. Allen, Jonathan Barrett, Dominic C. Horsman, Ciarán M. Lee, and Robert W. Spekkens. “Quantum common causes and quantum causal models”. *Phys. Rev. X* **7**, 031021 (2017).

[35] Eric G. Cavalcanti. “Classical causal models for bell and kochen-specker inequality viola-

tions require fine-tuning”. *Phys. Rev. X* **8**, 021018 (2018).

[36] Paweł Blasiak, Ewa Borsuk, and Marcin Markiewicz. “On safe post-selection for Bell tests with ideal detectors: Causal diagram approach”. *Quantum* **5**, 575 (2021).

[37] Valentin Gebhart, Luca Pezzè, and Augusto Smerzi. “Genuine multipartite nonlocality with causal-diagram postselection”. *Phys. Rev. Lett.* **127**, 140401 (2021).

[38] Bernard Yurke and David Stoler. “Bell’s-inequality experiments using independent-particle sources”. *Phys. Rev. A* **46**, 2229–2234 (1992).

[39] Bernard Yurke and David Stoler. “Einstein-podolsky-rosen effects from independent particle sources”. *Phys. Rev. Lett.* **68**, 1251–1254 (1992).

[40] J. D. Franson. “Bell inequality for position and time”. *Phys. Rev. Lett.* **62**, 2205–2208 (1989).

[41] Sven Aerts, Paul Kwiat, Jan-Åke Larsson, and Marek Z’ukowski. “Two-photon franson-type experiments and local realism”. *Phys. Rev. Lett.* **83**, 2872–2875 (1999).

[42] Jonathan Jogenfors, Ashraf Mohamed El-hassan, Johan Ahrens, Mohamed Bourennane, and Jan Åke Larsson. “Hacking the bell test using classical light in energy-time entanglement-based quantum key distribution”. *Sci. Adv.* **1**, e1500793 (2015).

[43] Adán Cabello, Alessandro Rossi, Giuseppe Vallone, Francesco De Martini, and Paolo Mataloni. “Proposed bell experiment with genuine energy-time entanglement”. *Phys. Rev. Lett.* **102**, 040401 (2009).

[44] G. Lima, G. Vallone, A. Chiuri, A. Cabello, and P. Mataloni. “Experimental bell-inequality violation without the post-selection loophole”. *Phys. Rev. A* **81**, 040101 (2010).

[45] George Svetlichny. “Distinguishing three-body from two-body nonseparability by a bell-type inequality”. *Phys. Rev. D* **35**, 3066–3069 (1987).

[46] N. David Mermin. “Extreme quantum entanglement in a superposition of macroscopically distinct states”. *Phys. Rev. Lett.* **65**, 1838–1840 (1990).

[47] Jean-Daniel Bancal, Cyril Branciard, Nicolas Gisin, and Stefano Pironio. “Quantifying multipartite nonlocality”. *Phys. Rev. Lett.* **103**, 090503 (2009).

[48] Jean-Daniel Bancal, Jonathan Barrett, Nicolas Gisin, and Stefano Pironio. “Definitions of multipartite nonlocality”. *Phys. Rev. A* **88**, 014102 (2013).